

Production of particle unstable light nuclei in 11.5 A GeV/c Au + Pt heavy-ion collisions

T.A. Armstrong,^(8,a) K.N. Barish,⁽³⁾ S. Batsouli,⁽¹³⁾ S.J. Bennett,⁽¹²⁾ M. Bertaina,^(7,b) A. Chikanian,⁽¹³⁾ S.D. Coe,^(13,c) T.M. Cormier,⁽¹²⁾ R. Davies,^(9,d) C.B. Dover,^(1,e) P. Fachini,⁽¹²⁾ B. Fadem,⁽⁵⁾ L.E. Finch,⁽¹³⁾ N.K. George,^(13,f) S.V. Greene,⁽¹¹⁾ P. Haridas,^(7,g) J.C. Hill,⁽⁵⁾ A.S. Hirsch,⁽⁹⁾ R. Hoversten,⁽⁵⁾ H.Z. Huang,⁽²⁾ H. Jaradat,⁽¹²⁾ B.S. Kumar,^(13,h) T. Lainis,⁽¹⁰⁾ J.G. Lajoie,⁽⁵⁾ R.A. Lewis,⁽⁸⁾ Q. Li,⁽¹²⁾ B. Libby,^(5,i) R.D. Majka,⁽¹³⁾ T.E. Miller,⁽¹¹⁾ M.G. Munhoz,⁽¹²⁾ J.L. Nagle,⁽⁴⁾ I.A. Pless,⁽⁷⁾ J.K. Pope,^(13,j) N.T. Porile,⁽⁹⁾ C.A. Pruneau,⁽¹²⁾ M.S.Z. Rabin,⁽⁶⁾ J.D. Reid,^(11,k) A. Rimai,^(9,l) A. Rose,⁽¹¹⁾ F.S. Rotondo,^(13,m) J. Sandweiss,⁽¹³⁾ R.P. Scharenberg,⁽⁹⁾ A.J. Slaughter,⁽¹³⁾ G.A. Smith,⁽⁸⁾ M.L. Tincknell,^(9,n) W.S. Toothacker,^(8,e) G. Van Buren,^(7,2,o) F.K. Wohn,⁽⁵⁾ Z. Xu⁽¹³⁾
(The E864 Collaboration)

⁽¹⁾ *Brookhaven National Laboratory, Upton, New York 11973*

⁽²⁾ *University of California at Los Angeles, Los Angeles, California 90095*

⁽³⁾ *University of California at Riverside, Riverside, California 92521*

⁽⁴⁾ *Columbia University, New York 10027*

⁽⁵⁾ *Iowa State University, Ames, Iowa 50011*

⁽⁶⁾ *University of Massachusetts, Amherst, Massachusetts 01003*

⁽⁷⁾ *Massachusetts Institute of Technology, Cambridge, Massachusetts 02139*

⁽⁸⁾ *Pennsylvania State University, University Park, Pennsylvania 16802*

⁽⁹⁾ *Purdue University, West Lafayette, Indiana 47907*

⁽¹⁰⁾ *United States Military Academy, West Point, New York 10996*

⁽¹¹⁾ *Vanderbilt University, Nashville, Tennessee 37235*

⁽¹²⁾ *Wayne State University, Detroit, Michigan 48201*

⁽¹³⁾ *Yale University, New Haven, Connecticut 06520*

(September 29, 2000)

We report measurements from experiment E864 at the BNL-AGS of the yields of particle unstable light nuclei in central collisions of ^{197}Au with beam momentum of 11.5 A GeV/c on ^{197}Pt . Yields are reported as a function of rapidity for the nuclei ^4H , ^4Li , ^5He , and ^5Li in the rapidity range from y_{cm} to $y_{cm} + 0.8$ and in the transverse momentum range of approximately $0.1 \leq p_T/A \leq 0.4\text{GeV}/c$. The yields are compared to previously reported yields and trends for production of particle stable light nuclei. The non-observation of two excited states $^5\text{He}_{16.75\text{MeV}}^*$ and $^5\text{Li}_{16.66\text{MeV}}^*$ is used to set an upper limit on the yields of these states.

25.75.-q

I. INTRODUCTION

Relativistic heavy ion collisions which are believed to reach energy densities many times greater than normal nuclear matter allow the examination of the strong interaction in a novel environment. In order to understand the dynamics of the collision system, one must use the only available tools - the species and momenta of the particles which exit the collision region. Because of the violence of heavy ion collisions, it is highly improbable for a nuclear cluster near center-of-mass rapidity ($y_{cm}=1.6$) in a collision at these energies to be a fragment of the beam or target nucleus [1]. This would involve a cluster suffering a momentum loss of several GeV/c per nucleon that does not destroy the cluster, which is typically bound by only a few MeV per nucleon. These nuclei then are formed by coalescence and so represent correlations of several nucleons. As the mass of measured nuclei increases so does the number of particles involved in the correlation and so does the sensitivity to features of the freeze-out distribution.

In part due to the fragility of these states, the observed light nuclei are believed to be formed only near freeze-out of the collision system, at which time the mean free path of a bound cluster is long enough for it to escape without further collision. We have previously reported measurements of yields of particle stable light nuclei up to $A=7$ in collisions of ^{197}Au with beam momentum of 11.5 A GeV/c on ^{197}Pt and ^{208}Pb targets and have discussed the trends of these measurements [2] [3] [4]. At AGS energies many measurements exist of particle spectra for single and composite hadrons in heavy ion collisions [5]. Measurements of the yields of particle unstable nuclei can provide further insight into the evolution of the collision environment. In this paper we present measurements of the yields of the particle unstable nuclei ^4H , ^4Li , ^5He , and ^5Li and limits for the yields of two excited states $^5\text{He}_{16.75\text{MeV}}^*$ and $^5\text{Li}_{16.66\text{MeV}}^*$

in the 10% most central collisions of ^{197}Au with beam momentum of 11.5 A GeV/c on ^{197}Pt . These are compared to the trends observed in the stable nuclei yields. We note that the widths of these unstable states (less than a few MeV/c^2) give lifetimes $c\tau \gtrsim 40\text{fm}$ which means most produced nuclei decay outside of the expected collision volume.

II. EXPERIMENT 864

A. Apparatus

E864 uses an open geometry two-dipole spectrometer designed for high sensitivity searches for exotic and rare composite objects. The apparatus (Fig. 1) has been described in detail elsewhere [6], so only the key items for this analysis will be described here. The 11.5 A GeV/c beam of Au ions is incident on a 1.5cm thick Pt target (60% IL for Au). Beam definition counters and a scintillation multiplicity array [7] near the target form the first level trigger for the experiment. Downstream of the dipole magnets, scintillation counter hodoscopes, and straw tube arrays [8] provide TOF, dE, and position measurements which allow offline calculation of the charge, velocity, and rigidity of charged particles and thus the mass, momentum, and species. A highly segmented scintillating fiber and lead hadronic calorimeter [9] at the downstream end of the experiment allows an independent measurement of TOF and energy for charged particles and identification of neutral particles. The tower-by-tower correlated TOF and energy from the calorimeter are used to make a second level high mass trigger (LET) [10]. The LET trigger can reject interactions with no high mass particle in the spectrometer by a factor of 50 - 70.

Data from two separate runs are used for the analysis presented here. For both sets the first level trigger selected the 10% most central interactions. A large data sample was recorded at the highest spectrometer field (1.5T) with a primary goal of searching for strange quark matter. At this field setting the majority particles (p, π) are swept out of the spectrometer aperture. There is still moderate acceptance for ^4He and ^3H ions and good acceptance for neutrons. With these settings 250×10^6 LET triggers were recorded which sampled 13×10^9 10% most central interactions. This set of data is used for the ^4H and ^5He measurements. A second set of data was recorded at a lower field setting (0.45T) with good acceptance for protons and all light ions. At this setting 45×10^6 LET triggers were recorded which sampled 1.9×10^9 10% most central interactions. This data set is used for the ^4Li , ^5Li , and excited state analysis.

B. Data Analysis

Single particle species are identified by using the charge and mass calculated from rigidity, dE, and TOF for charged particles and the mass calculated from the TOF and energy in the calorimeter for neutral particles. Details of the particle identification and resolution are given in previous papers [2] [3] [6]. The particle unstable nuclei are identified by their decay into two daughter particles:

$$^4\text{H} \rightarrow ^3\text{H} + n$$

$$^4\text{Li} \rightarrow ^3\text{He} + p$$

$$^5\text{He} \rightarrow ^4\text{He} + n$$

$$^5\text{Li} \rightarrow ^4\text{He} + p$$

$$^5\text{He}_{16.75\text{MeV}}^* \rightarrow ^3\text{H} + d$$

$$^5\text{Li}_{16.66\text{MeV}}^* \rightarrow ^3\text{He} + d$$

For a given unstable nucleus events are selected which have at least one identified daughter of each type. Both particles are required to pass track or shower quality cuts and be consistent with coming from the target within the experiment's aperture. All pairs are used to calculate an invariant mass spectrum. Since most entries in this spectrum are uncorrelated background, one must determine the shape of the background spectrum. This is done by combining daughter particles of one type from one event with daughter particles of the other type from another event (event mixing). An additional cut requires the particles of a pair in both the same event spectrum and the mixed event spectrum to be separated by more than the two-track resolution in the relevant detectors. For charged pairs the cut was adjusted to be well beyond the observed two-track resolution in the tracking detectors. For pairs with one charged and one neutral particle, the neutral particle was required to be on one side of the detector (horizontally) and the charged particle on the other side with the two sides assigned to give optimum efficiency for simulated decays and

the separation between the two sides larger than the two shower resolution in the calorimeter. This assures that the mixed event spectrum will not include pairs which could not be found if both tracks were in the same event.

The mixed event spectrum is then normalized to the same event spectrum to extract the signal in two ways. In the first method the mixed event spectrum is normalized to the same event spectrum in a mass region above the expected signal. For the second method, Monte Carlo generated resonance decays are simulated through the entire apparatus and reconstructed. Then a linear combination of the Monte Carlo spectrum plus the mixed event spectrum is fitted to the same event spectrum and the normalization parameter from the fit is used to scale the mixed event spectrum. For both methods the normalized mixed event spectrum is subtracted from the same event spectrum and the subtracted spectrum is then integrated over the region of the expected signal. For the results presented in this paper, the two methods agree well within statistical error. Figure 2 shows the ${}^5\text{Li}$ same event pair spectrum and mixed event pair spectrum overlaid as well as the subtracted spectrum with the Monte Carlo spectrum overlaid. The normalization for the mixed event spectrum and the Monte Carlo spectrum is from the linear fit described above. The plot includes data from the entire rapidity range ($1.6 \leq y \leq 2.4$) to minimize statistical error so finer binning can be used to compare the shapes. We note that the signal width in Fig. 2 is dominated by our resolution.

For pairs where both particles are charged the mixed event spectrum is modified to simulate the Coulomb interaction of the pair so it will be canceled by the subtraction. The form of the Coulomb interaction is taken to be a simple formula suggested by Baym and Braun-Munzinger [11]:

$$\frac{q^2}{2m_{red}} = \frac{q_o^2}{2m_{red}} + \frac{Z_1 Z_2}{r_o} \quad (1)$$

where q_o is the measured relative momentum of the pair, q is the modified relative momentum, m_{red} is the reduced mass, and Z_1 and Z_2 are the charges of the two particles. We set the one parameter r_o which accounts for the average distance between the particles in the pair at freeze out from the deuteron-proton invariant mass spectrum where no other significant correlations are expected. Figure 3 shows the subtracted deuteron-proton invariant mass spectrum with and without the Coulomb correction. We note that the shape in Fig. 3a is dominated by our resolution. Modification to the subtracted spectrum from the Coulomb interaction of the particles in a pair with the field of all the other particles is ignored. This interaction affects the single particle distributions and should largely cancel in the subtraction. Although other treatments of the Coulomb correction have been published, ([12] for example) this simple parameterization is adequate for the analysis presented here.

Mass spectra are made for all rapidity bins with enough data to see a signal. Due to the limited statistics, data are combined over a transverse momentum range of approximately $0.1 \leq p_T/A \leq 0.4 \text{ GeV}/c$. To compare the yield of unstable nuclei ($Y_{unstable}$) to the yield of the species of the heavy decay daughter (Y_{Heavy}) we measure the number per event $N(y, p_t)$ of each in a given rapidity bin (Δy) and in a p_t range (Δp_t) centered about (y, p_t) . The invariant multiplicity is given by:

$$Y(y, p_t) = \frac{1}{2\pi p_t} \frac{N(y, p_t)}{\Delta p_t \Delta y} \quad (2)$$

The ratio is given by:

$$\frac{Y_{unstable}(y, p_t)}{Y_{Heavy}(y, p_t^*)} = \frac{N_{unstable}(y, p_t)}{N_{Heavy}(y, p_t^*)} \left(\frac{m_{Heavy}}{m_{unstable}} \right)^2 \frac{1}{accept(y, p_t) * effic(y, p_t) * \eta_{tag}} \quad (3)$$

where $accept(y, p_t)$ and $effic(y, p_t)$ are the acceptance and efficiency for the light daughter when the heavy daughter has been accepted and the unstable parent is in the bin (y, p_t) . The p_t bin width and center for the heavy decay daughter, p_t^* , Δp_t^* , are scaled from those of the unstable parent by the ratios of the masses of the two nuclei so as to compare yields at similar transverse velocities. Finally, η_{tag} is the calculated target absorption for the light daughter. In this ratio, the trigger efficiency, acceptance, and detector efficiency of the heavy decay daughter cancel.

Table I shows the acceptance for ${}^5\text{Li}$ decays in the kinematic range accessible for the 0.45T spectrometer field setting. Also shown is the acceptance for ${}^5\text{Li}$ decays when the decay ${}^4\text{He}$ is in the region of the calorimeter used for the Level II trigger for this data set. These values are typical for the acceptance for the unstable nuclei reported here.

For charged light daughters the efficiency includes detector and cut efficiencies (from data ≈ 0.8) and occupancy efficiency due to loss of the light daughter from overlapping tracks (from Monte Carlo tracks embedded in real events ≈ 0.7). For neutral light daughters (neutrons), the combination of cut efficiencies and loss due to overlapping showers in the calorimeter is calculated from embedding simulated showers in a real event (≈ 0.3 combined efficiency). A correction is made using the Monte Carlo resonance shape for loss of signal outside the mass region used for the signal which varies from $\approx 5\%$ in the lowest rapidity bin to $\approx 10\%$ in the highest rapidity bin. For the $A=5$ ground states, a correction is also made for ${}^3\text{He}$ contamination of the ${}^4\text{He}$ by extrapolating the ${}^3\text{He}$ shape under the ${}^4\text{He}$ peak. This

correction is field and rapidity dependent, varying from less than 1% in the low rapidity bin ($1.6 \leq y \leq 1.8$) to 16% at the high rapidity bin ($2.2 \leq y \leq 2.4$). All these corrections are calculated as a function of rapidity and in the same p_T/A range used for the analysis.

Systematic errors that we have characterized include variation of the calculated acceptance with assumed production model ($\pm 10\%$ in the lowest rapidity bin to $\pm 3\%$ in the highest), uncertainty in the correction for contamination of ${}^4\text{He}$ by ${}^3\text{He}$ for ${}^5\text{He}$ and ${}^5\text{Li}$ (only significant in the highest rapidity bin - $\pm 8\%$), and uncertainty in the Coulomb correction for charged pairs ($\pm 5\%$ to $\pm 15\%$ depending on species and rapidity bin). For ${}^4\text{Li}$ and ${}^4\text{H}$ we note that the width of the reconstructed invariant mass peaks are narrower than the value given in ref. [13]. For example, for ${}^4\text{Li}$ the width that we observe is consistent with our resolution for a zero width peak ($\approx 3.5 \text{ MeV}/c^2$ fwhm). We conclude that the width is less than $\approx 3 \text{ MeV}/c^2$ which is consistent with other measurements (e.g. [14], [15]). The value of this width slightly affects the acceptance and the correction for signal lost outside the mass region integrated to count the signal. For the ${}^4\text{Li}$ results presented here, a width of $2 \text{ MeV}/c^2$ is used, and an additional systematic error of $\pm 3 - 5\%$ is included which covers a possible variation in width from 1 to $3 \text{ MeV}/c^2$. For the data presented here, the total estimated systematic error is added in quadrature to the statistical error. No corrections have been made for possible contributions to the mass peaks from excited states. We note that if these higher states are produced just in proportion to their spin factors, then they would represent $\approx 50 - 60\%$ of the measured $A=4$ yield and $\approx 13 - 17\%$ of the measured $A=5$ yield.

For the two excited states where we see no signal the total error, including statistical errors, systematic errors, and errors on the branching ratios [16] [17] added in quadrature, is used to estimate a 90% confidence level upper limit for the yields.

III. RESULTS AND DISCUSSION

The ratios of invariant multiplicities for ${}^4\text{H}/{}^3\text{H}$, ${}^4\text{Li}/{}^3\text{He}$, ${}^5\text{He}/{}^4\text{He}$, and ${}^5\text{Li}/{}^4\text{He}$ are shown in Fig. 4 and Fig. 5. We use the previously reported invariant multiplicities [2] to convert these ratios to the invariant multiplicities shown in Fig. 6 and Fig. 7. Included in Fig. 6 for comparison are the invariant multiplicities for ${}^4\text{He}$ from ref. [2] averaged over the p_T range used here. Also shown in Fig. 7 are the 90% confidence level upper limits for the two $A=5$ ($3/2^+$) excited states. The ratios and calculated multiplicities and errors are also given in table II.

Some interesting features are evident from these figures. The invariant multiplicities for the $A=4$ unstable nuclei are within 50% of the invariant multiplicity for ${}^4\text{He}$ even though the spin factor for the unstable nuclei is five ($J=2$) while it is only one ($J=0$) for ${}^4\text{He}$. There are no stable $A=5$ nuclei to compare with the unstable states, but they can be compared to the trends observed for the stable nuclei. Figure 8 shows the invariant multiplicities for ten stable nuclei at low p_t ($p_t/A \leq 300 \text{ MeV}/c$) and $1.8 \leq y \leq 2.0$ [2] along with the measurements for the four unstable nuclei and limits for the two excited states reported here. All multiplicities in this figure have been divided by $(2J+1)/2$ (spin factor normalized to proton) so as to allow a more direct comparison. The $A=7$ points which were measured in different rapidity bins have been shifted by a correction factor extrapolated from the rapidity shapes of the lighter nuclei ($\times 0.61$ for ${}^7\text{Li}$ and $\times 0.90$ for ${}^7\text{Be}$). The exponential curve is fitted to the stable nuclei. The unstable nuclei follow the general exponential fall with increasing A that is seen in the stable nuclei, but are significantly below the level indicated by the fitted exponential. Since the mass difference between the stable and unstable $A=4$ nuclei ($\approx 23 \text{ MeV}$) is small compared to the temperatures of these collisions at freeze out ($\approx 100 \text{ MeV}$ or greater) [18], a thermal model [20] would lead one to expect that the yields (scaled by the spin factor) would be similar. Thermal models generally give yields integrated over kinematic variables but our measurements are over a certain range in rapidity and p_T . Given the large difference when corrected for spin factor between the stable and unstable $A=4$ multiplicities however, and the fact that the ratios of the unstable to stable states vary by less than 25% from their average over the large rapidity region covered, it is not possible to ascribe the difference to the high p_t region not measured in our experiment.

The yield of the $A=5$ excited states are significantly below the ground state yields. In many lower energy experiments, the ratio of yields of these excited states to the ground states has been used to determine the temperature of the system produced in the collision [19]. This method is not expected to be valid when the temperature is much greater than the excitation energy of the excited state. It is interesting to note however that the upper limits on the production of the two $A=5$ excited states would imply a temperature lower than 7-13 MeV ($y=2.3 - y=1.9$) if interpreted in this way. Since temperatures at these energies have been previously measured to be $\approx 100 \text{ MeV}$ or greater, a more consistent interpretation of the lower yields of excited and unstable states may come from a coalescence model such as that of Heinz and Scheibl [21] which explicitly includes the internal structure of the formed cluster.

IV. SUMMARY

We have measured the yields of four unstable nuclei, ${}^4\text{H}$, ${}^4\text{Li}$, ${}^5\text{He}$, and ${}^5\text{Li}$ in 11.5 A GeV/c Au + Pt 10% most central collisions in the rapidity range from y_{cm} to $y_{cm} + 0.8$ and in the transverse momentum range of approximately $0.1 \leq p_T/A \leq 0.4\text{GeV}/c$. The invariant multiplicities in this kinematic range fall significantly below what would be expected from a simple thermal model based on the previously measured yields of particle stable nuclei.

V. ACKNOWLEDGEMENTS

We gratefully acknowledge the efforts of the AGS staff in providing the beam. This work was supported in part by grants from the Department of Energy (DOE) High Energy Physics Division, the DOE Nuclear Physics Division, and the National Science Foundation.

-
- ^a Present address: Vanderbilt University, Nashville, Tennessee 37235
^b Present Address: Istituto di Cosmo-Geofisica del CNR, Torino, Italy / INFN Torino, Italy
^c Present Address: Anderson Consulting, Hartford, CT
^d Present address: Univ. of Denver, Denver CO 80208
^e Deceased.
^f Present address: Argonne National Laboratory, 9700 S. Cass Ave., Argonne, Illinois 60439
^g Present address: Cambridge Systematics, Cambridge, MA 02139
^h Present address: McKinsey & Co., New York, NY 10022
ⁱ Present address: Department of Radiation Oncology, Medical College of Virginia, Richmond VA 23298
^j Present address: University of Tennessee, Knoxville TN 37996
^k Present address: Geology and Physics Dept., Lock Haven University Lock Haven, PA 17745
^l Present address: Institut de Physique Nucléaire, 91406 Orsay Cedex, France
^m Present Address: Institute for Defense Analysis, Alexandria VA 22311
ⁿ Present Address: MIT Lincoln Laboratory, Lexington MA 02420-9185
^o Present address: Brookhaven National Laboratory, Upton, New York 11973
- [1] L. C. Alexa *et al.*, Phys. Rev. Lett. **82**, 1374(1999); D. Abbott *et al.*, Phys. Rev. Lett. **82**, 1379(1999).
[2] T. A. Armstrong *et al.*, Phys. Rev. **C61**, 064908-1(2000).
[3] T. A. Armstrong *et al.*, Phys. Rev. **C60**, 064903-1(1999).
[4] T. A. Armstrong *et al.*, Phys. Rev. Lett. **83**, 5431(1999).
[5] *Heavy Ion Physics From Bevalac To RHIC, Proceedings of the Relativistic Heavy Ion Symposium, APS Centennial Meeting '99*, Atlanta, 1999, edited by R. Seto (World Scientific, Singapore)
[6] T. A. Armstrong *et al.*, Nucl. Inst. Meth. **A437**, 222(1999).
[7] P. Haridas, I. A. Pless, G. Van Buren, J. Tomasi, M. S. Z. Rabin, K. Barish and R. D. Majka, Nucl. Inst. Meth. **A385**, 413(1997).
[8] T. A. Armstrong, R. A. Lewis, J. Passaneau, G. A. Smith, J. D. Reid, J. Stell and W. S. Toothacker, Nucl. Instrum. Meth. **A425**, 210 (1999).
[9] T. A. Armstrong, *et al.*, Nucl. Inst. Meth. **A406**, 227(1998).
[10] J. C. Hill *et al.*, Nucl. Inst. Meth. **A421**, 431(1999).
[11] G. Baym and P. Braun-Munzinger, Nucl. Phys. **A610**, 286C(1996).
[12] Scott Pratt, Phys. Rev. **D33**, 72(1985).
[13] *Table of Isotopes, Eight Edition*, edited by Richard B. Firestone and Virginia S. Shirley (John Wiley & Sons, Inc., New York, 1996)
[14] M. Bruno, C. Cannata, M. D'Agotino and M. L. Fiandri, Phys. Rev. **C42**, 448(1990).
[15] B. Brinkmoller, H. P. Morsch, P. Decowski, M. Rogge, R. Siebert and P. Turek, Phys. Rev. **C42**, 550(1990).
[16] D. R. Tilley, H. R. Weller and G. M. Hale, Nucl. Phys. **A541**, 1(1992).
[17] B. Haesner, W. Heeringa, H. O. Klages, H. Dobiach, G. Schmalz, P. Schwarz, J. Wilczynski and B. Zeitnitz, Phys. Rev. **C28**, 995(1983).
[18] see for example P. Braun-Munzinger and J. Stachel, Nucl. Phys. **A606**, 320(1996) and references therein.
[19] see for example C. Schwarz *et al.*, Phys. Rev. **C48**, 676(1993); J. B. Natowitz, J. C. Hagel, R. Wada, X. Bin, J. Li, Y. Lou, and D. Utley, Phys. Rev. **C48**, 2074(1993) and references therein.

- [20] S. Das Gupta and A. Z. Mekjian, *Physics Reports*, **72**,131(1981), P. Braun-Munzinger, J. Stachel, J. P. Wessels, and N. Xu, *Phys. Phys. Lett.* **B 344**, 43(1995).
- [21] R. Scheibl and U. Heinz, *Phys. Rev.* **C59**, 1585(1999).

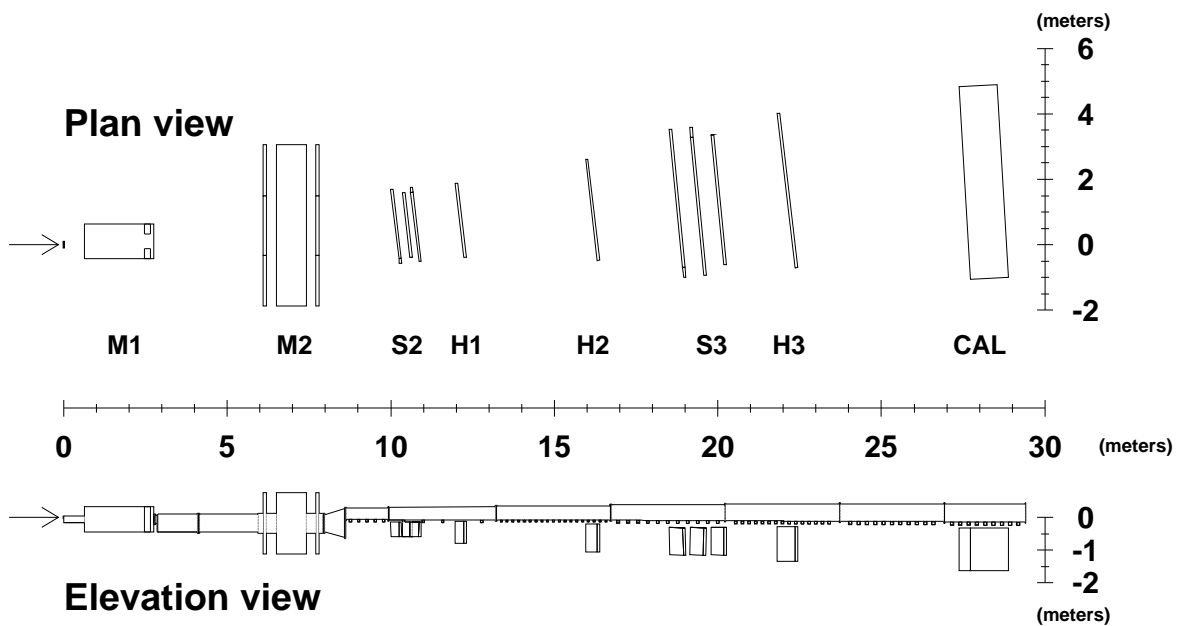


FIG. 1. The E864 spectrometer in plan and elevation views, showing the dipole magnets (M1 and M2), hodoscopes (H1, H2, and H3), straw tube arrays (S2 and S3) and hadronic calorimeter (CAL). The vacuum chamber is not shown in the plan view.

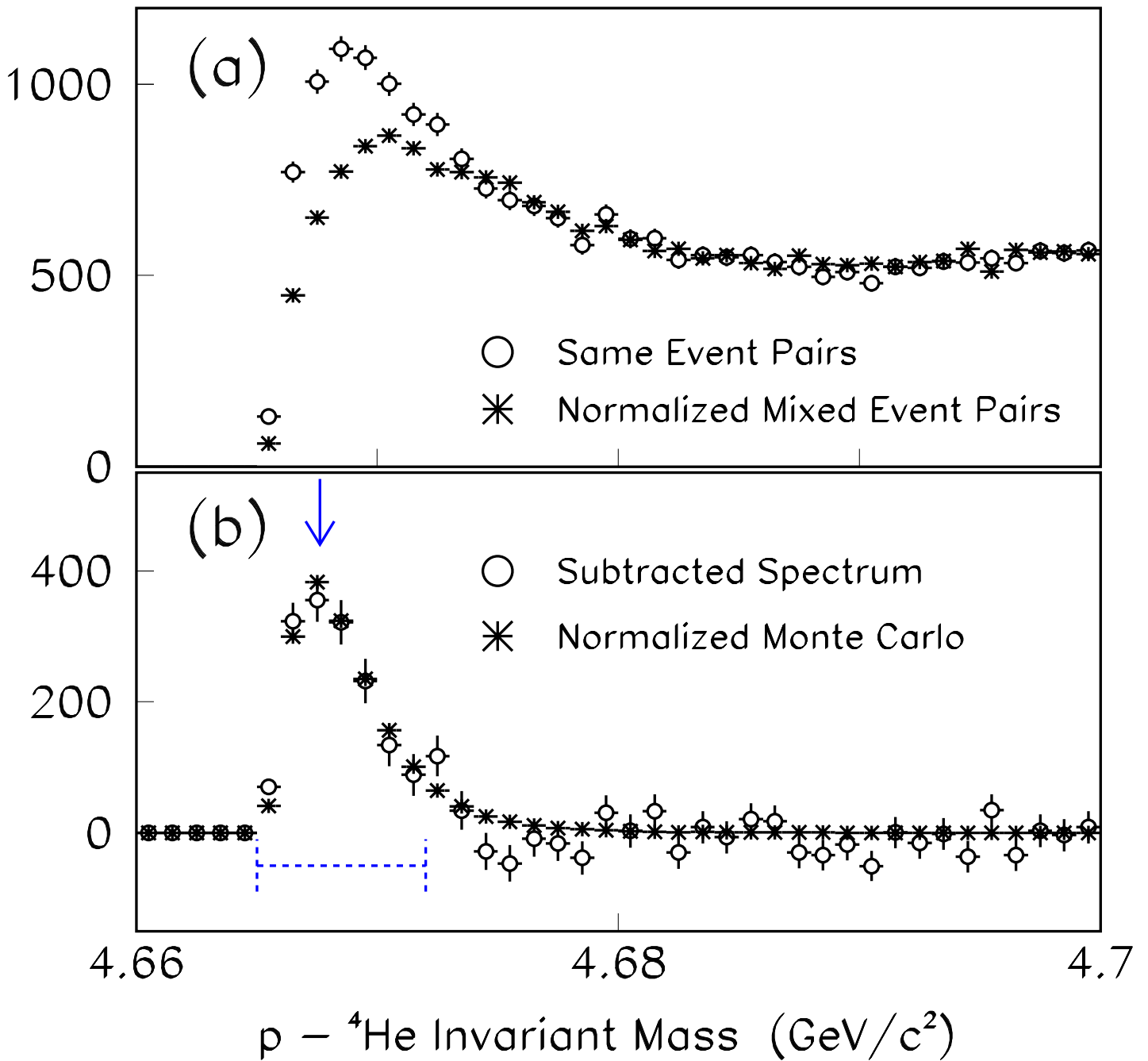


FIG. 2. Example of mixed event analysis. Panel (a) shows the invariant mass spectrum for same event $p - {}^4\text{He}$ pairs (open circles) and mixed event pairs (asterisks) with a correction to simulate the Coulomb interaction. Panel (b) shows the subtracted spectrum (open circles) and the Monte Carlo simulated signal for ${}^5\text{Li}$ (asterisks). The mixed event and Monte Carlo spectra are normalized with the parameters from a linear fit to the same event spectrum as described in the text. The arrow shows the nominal ${}^5\text{Li}$ mass. The dashed lines show the region integrated to measure the signal. The plots include data from the full rapidity range to decrease the statistical error so that fine binning may be used to see the shapes.

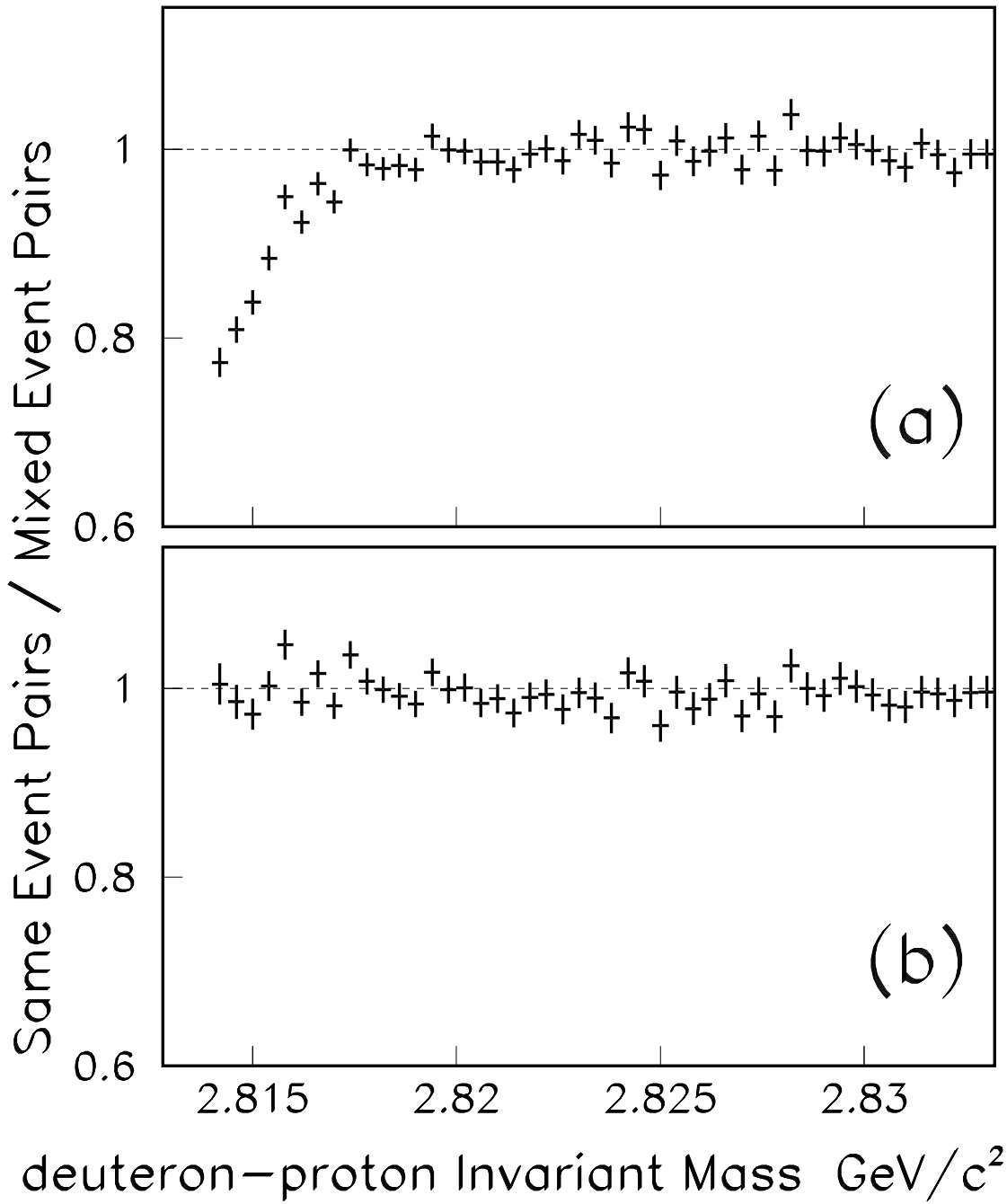


FIG. 3. Determination of the Coulomb correction from the deuteron-proton invariant mass spectrum. Panel (a) shows the ratio of the same event to mixed event mass spectrum with no correction. Panel (b) shows the same with the Coulomb correction.

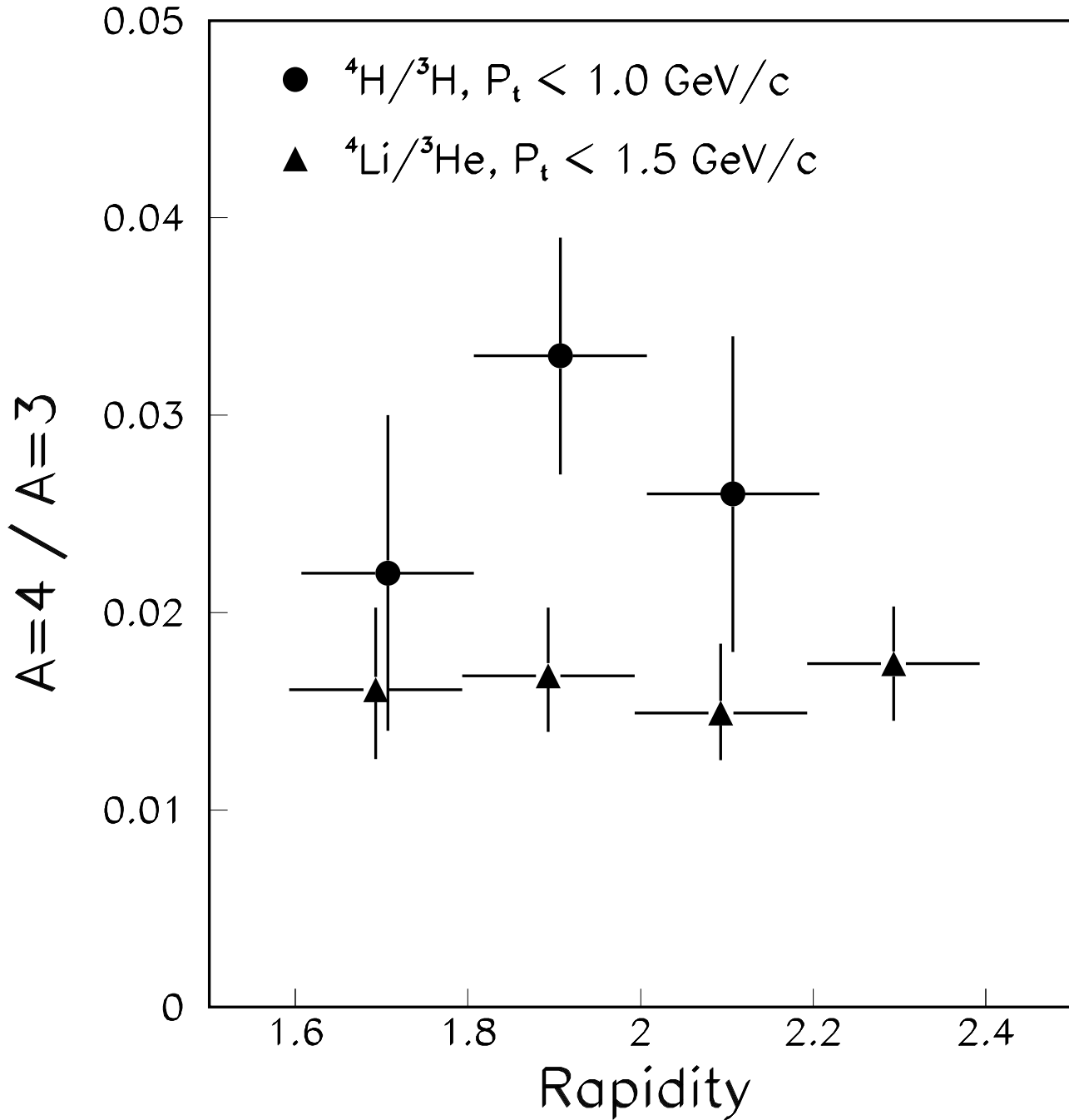


FIG. 4. Ratios of invariant multiplicities of $A=4$ unstable nuclei to invariant multiplicities of the heavy decay daughter species. (Data points for different species are offset slightly from rapidity bin centers for clarity.)

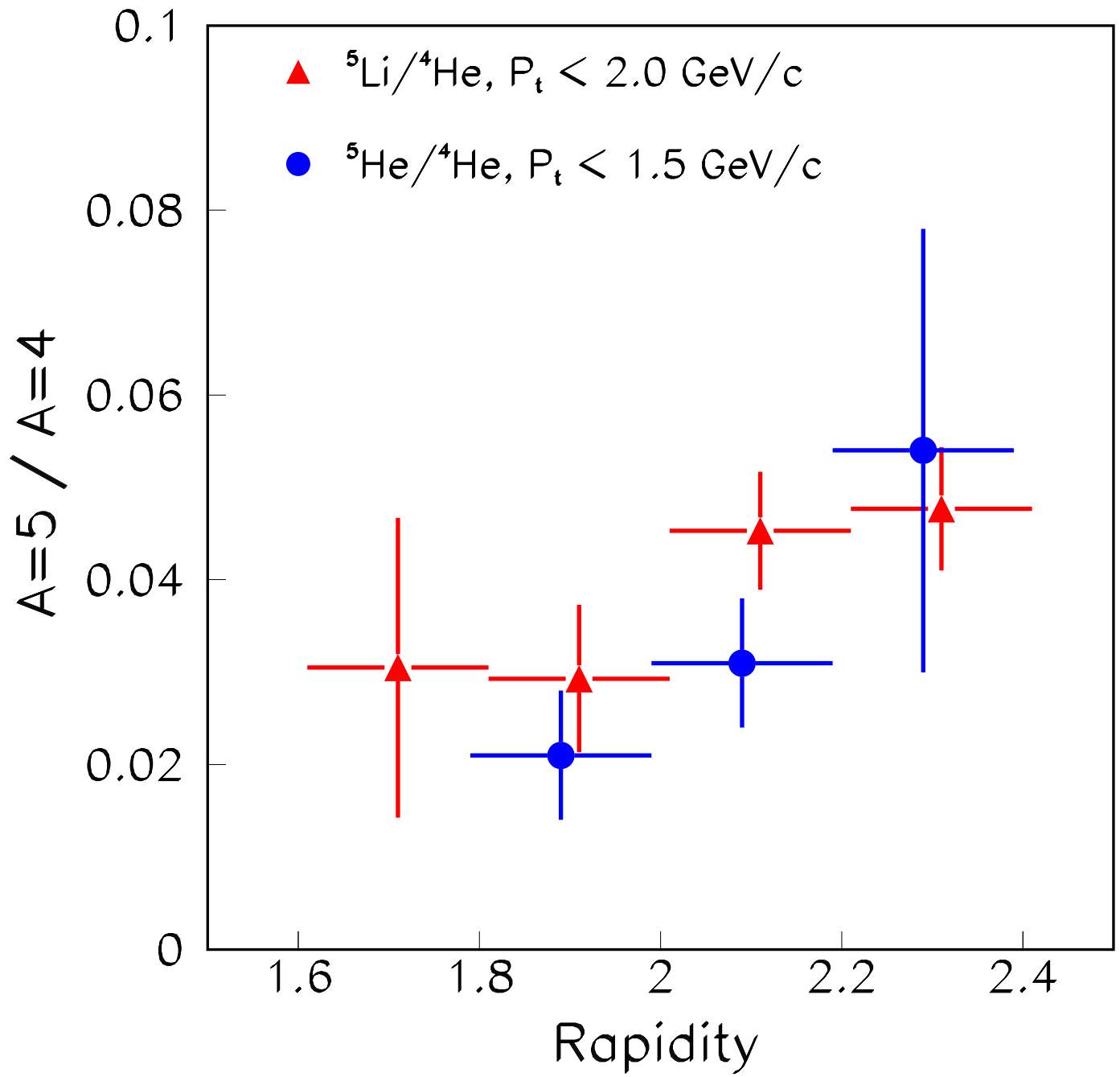


FIG. 5. Ratios of invariant multiplicities of $A=5$ unstable nuclei to invariant multiplicities of the heavy decay daughter species. (Data points for different species are offset slightly from rapidity bin centers for clarity.)

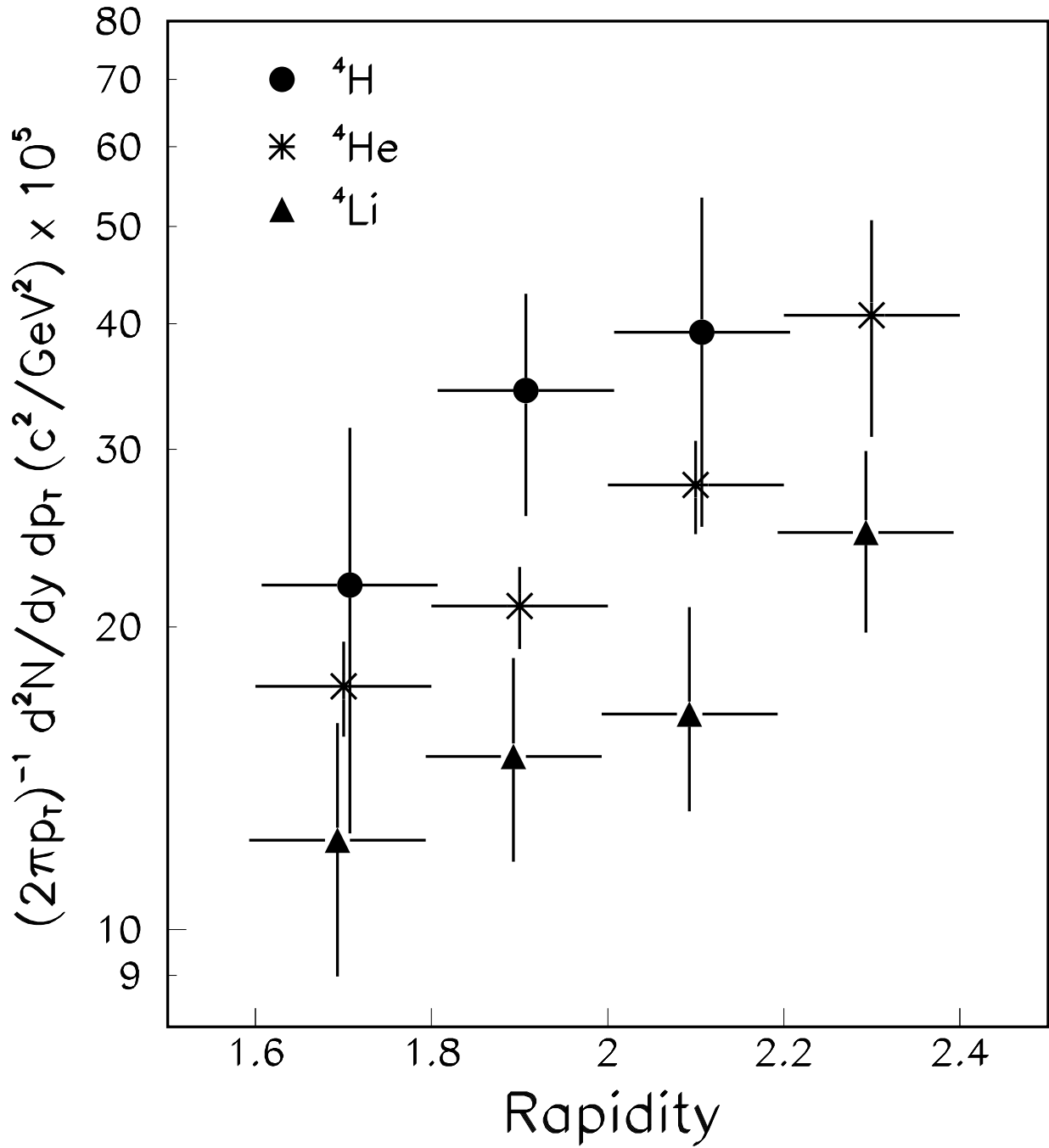


FIG. 6. Invariant multiplicities of $A=4$ nuclei. (Data points for different species are offset slightly from rapidity bin centers for clarity.)

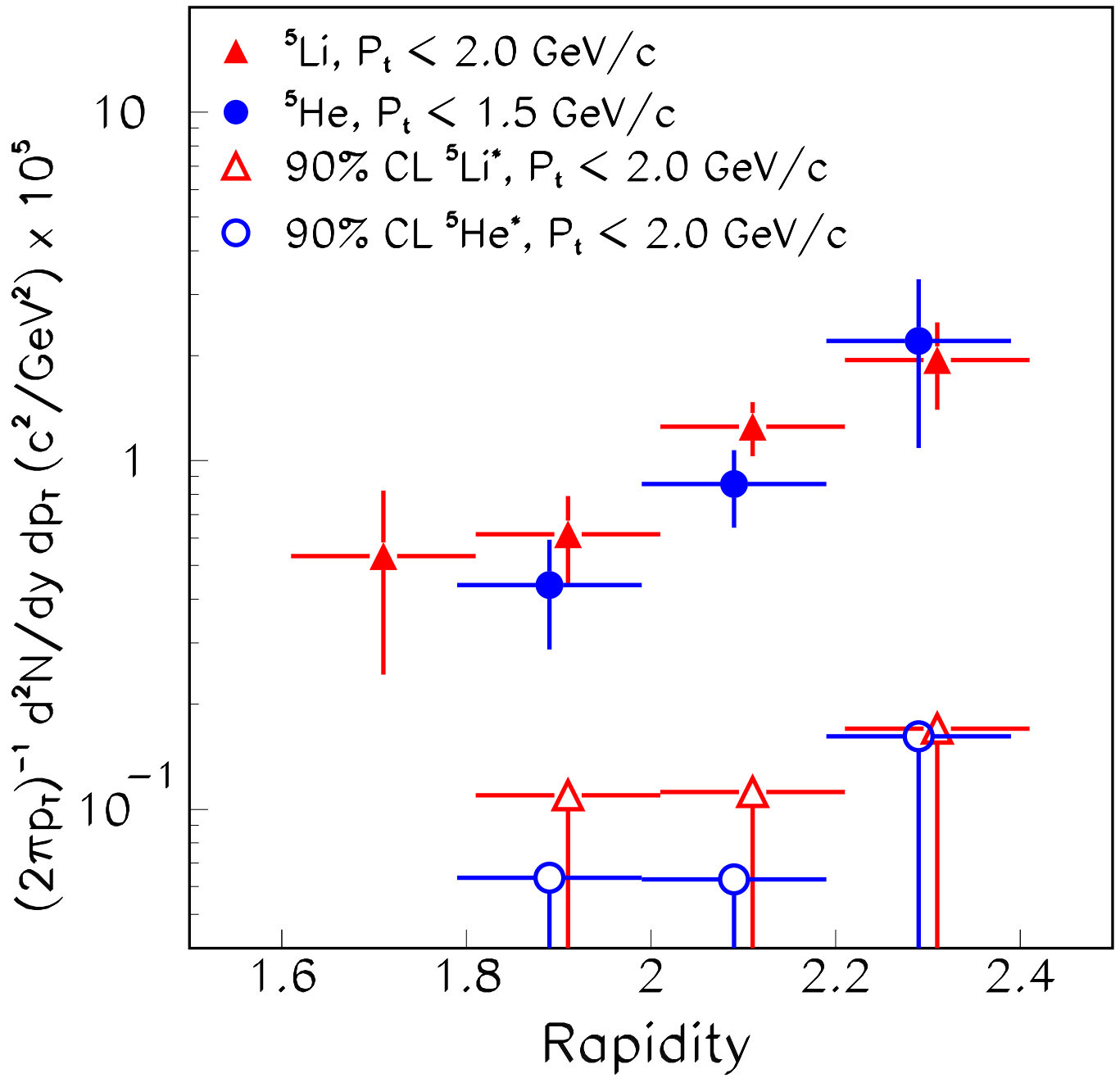


FIG. 7. Invariant multiplicities of $A=5$ nuclei and upper limits for the two excited states. (Data points for different species are offset slightly from rapidity bin centers for clarity.)

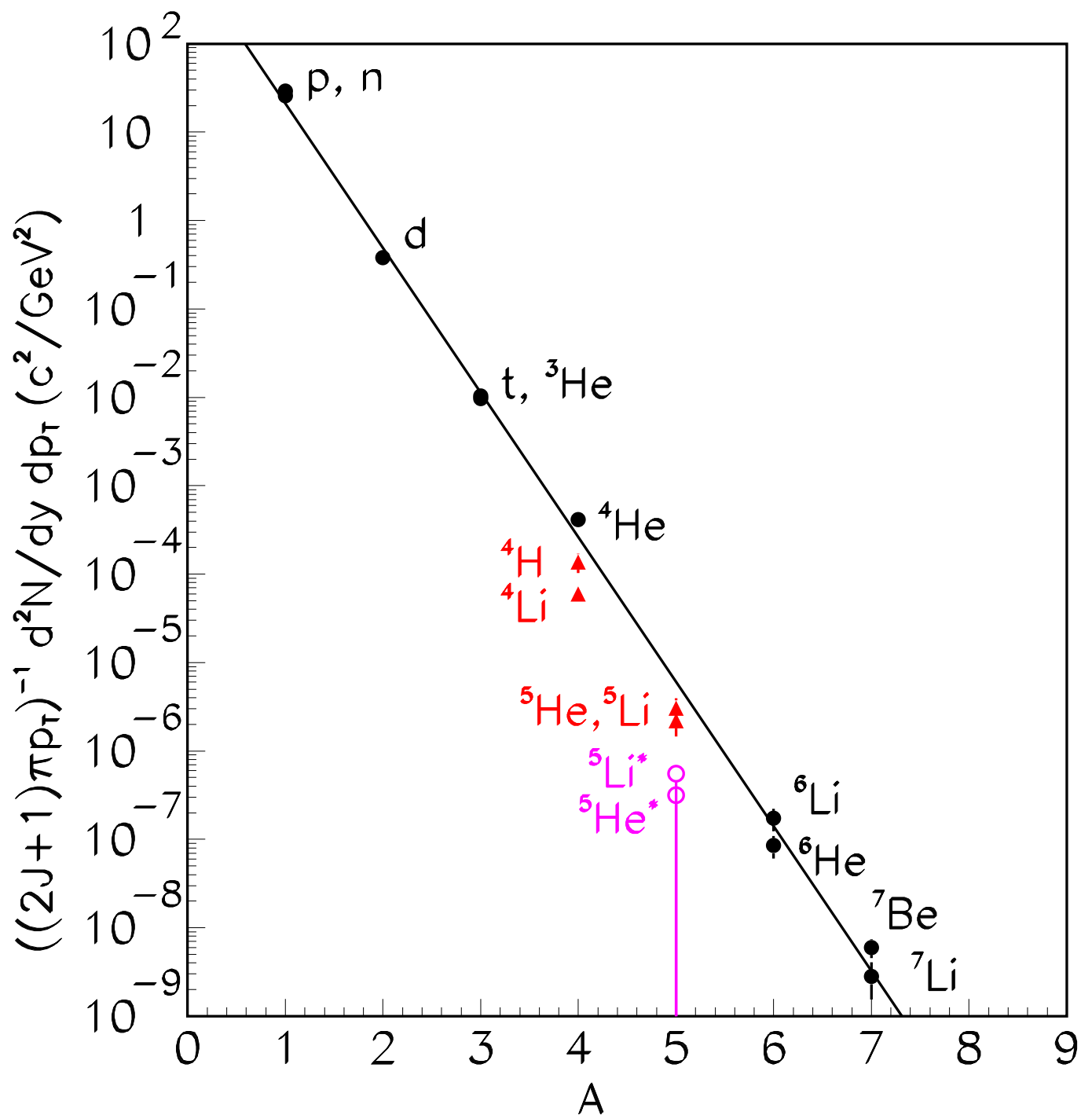


FIG. 8. Invariant multiplicities divided by $(2J+1)/2$ for stable and unstable nuclei in the range $1.8 \leq y \leq 2.0$. For the unstable nuclei and ${}^6\text{He}$, $p_t/A \leq 400\text{MeV}/c$. For the remaining nuclei, $p_t/A \leq 300\text{MeV}/c$. The curve is an exponential fitted to the particle stable nuclei.

TABLE I. Acceptances in per cent for ${}^5\text{Li}$ decays with a magnetic field of 0.45 T. The first line is total acceptance. The second line is the acceptance for a ${}^5\text{Li}$ decay when the ${}^4\text{He}$ is inside the calorimeter trigger region. These are typical of the acceptance for the data reported here.

	Rapidity	1.7	1.9	2.1	2.3
Acceptance (%) for ${}^5\text{Li}$		1.8	4.4	7.7	10.0
Acceptance (%) for ${}^5\text{Li}$ when ${}^4\text{He}$ is in the calorimeter trigger region		26.1	43.7	61.7	73.0

TABLE II. Ratios of the invariant multiplicity of the unstable nucleus to the invariant multiplicity of the species of its heavy decay daughter and the invariant multiplicities calculated using previously reported yields for the species of the heavy decay daughter. For the excited states, ${}^5\text{He}_{16.75\text{MeV}}^*$ and ${}^5\text{Li}_{16.66\text{MeV}}^*$ the 90% confidence level upper limit is given.

Rapidity	Ratios to heavy decay daughter			
	1.7	1.9	2.1	2.3
${}^4\text{Li}/{}^3\text{He}$	0.016 ± 0.004	0.017 ± 0.003	0.015 ± 0.003	0.017 ± 0.003
${}^4\text{H}/{}^3\text{H}$	0.022 ± 0.008	0.033 ± 0.006	0.026 ± 0.008	
${}^5\text{Li}/{}^4\text{He}$	0.031 ± 0.017	0.029 ± 0.008	0.045 ± 0.007	0.048 ± 0.009
${}^5\text{He}/{}^4\text{He}$		0.021 ± 0.007	0.031 ± 0.007	0.054 ± 0.021
	Invariant Multiplicities $\times 10^5 (c^2/\text{GeV}^2)$			
${}^4\text{Li}$	12 ± 2	15 ± 2	16 ± 1	25 ± 2
${}^4\text{H}$	22 ± 10	34 ± 9	39 ± 14	
${}^5\text{Li}$	0.53 ± 0.29	0.61 ± 0.18	1.3 ± 0.2	1.9 ± 0.5
${}^5\text{He}$		0.44 ± 0.15	0.86 ± 0.21	2.2 ± 1.1
${}^5\text{Li}_{16.66\text{MeV}}^*$ (90% CL upper limit)		0.11	0.11	0.17
${}^5\text{He}_{16.75\text{MeV}}^*$ (90% CL upper limit)		0.06	0.06	0.16